THESIS

EFFECTS OF HYDRAULIC STRUCTURES ON FISH PASSAGE: AN EVALUATION OF 2D VS 3D HYDRAULIC ANALYSIS METHODS

Submitted by

Erin R. Ryan

Department of Civil and Environmental Engineering

In partial fulfillment of the requirements

For the Degree of Master of Science

Colorado State University

Fort Collins, Colorado

Summer 2015

Master's Committee:

Advisor: Brian P. Bledsoe

Christopher A. Myrick
Peter A. Nelson

ABSTRACT

EFFECTS OF HYDRAULIC STRUCTURES ON FISH PASSAGE: AN EVALUATION OF 2D VS 3D HYDRAULIC ANALYSIS METHODS

Channel-spanning hydraulic structures can act as barriers to upstream fish movement. Negative consequences associated with this disruption of longitudinal habitat connectivity highlight the need for accurate and practicable assessment techniques. Three-dimensional evaluation methods have been shown to resolve the complex flow at in-stream structures and accurately predict fish movement; yet three-dimensional modeling can be impractical due to time and resource requirements. This study investigates using a two-dimensional computational fluid dynamics model and statistical analyses to describe the hydraulic conditions at a whitewater park structure in Lyons, Colorado. Fish movement observations are paired with the resulting hydraulic variables along spatially explicit, continuous paths which represent potential swimming routes. Logistic regression analyses indicate that flow depth and velocity are strongly associated with fish passage; a combined depth and velocity variable accurately predicts 92% of rainbow trout (*Oncorhynchus mykiss*) and brown trout (*Salmo trutta*) movement observations at this hydraulic structure. The results of this study suggest that two-dimensional analysis methods can provide a cost-effective approach to assessing the effects of similar hydraulic structures on fish passage when three-dimensional analysis in not feasible. Further, conclusions from this study can be used to guide management and design decisions for both trout and fishes with comparatively lower swimming performance.

ACKNOWLEDGEMENTS

I would like to thank Tim Stephens, Nell Kolden, and Brian Fox for their previous work from which I built upon with this study; my advisor, Dr. Brian Bledsoe, for his research guidance and support for my scientific pursuits; and my committee members Dr. Christopher Myrick and Dr. Peter Nelson for their advice throughout this study and my associated coursework. I would like to thank Matt Kondratieff and Colorado Parks and Wildlife (CPW) for their continued financial support for and enthusiastic interest in fish passage studies. Finally, I would like to thank my friends, family, and fellow graduate students for their willingness to discuss ideas, sharing of expertise, and overall encouragement.

TABLE OF CONTENTS

LIST OF TABLES

LIST OF FIGURES

LIST OF SYMBOLS

BD	body depth
H	flow depth
k_s	bed roughness parameter
q_x, q_y	x and y discharge intensity, respectively
rms	root-mean-square
TiW	height of caudal fin
TL	total length
U, V	x and y components of velocity, respectively
v_{burst}	velocity associated with the burst swimming capability of a fish
v_{fluc}	proxy variable for turbulence to describe velocity fluctuations in space
v_{rms}	average rms velocity between two points
x	streamwise directional plane
y	lateral directional plane
σ	standard deviation

UNITS OF MEASURE

BL	body length(s)
BL/s	body length(s) per second
cms	cubic meters per second
%	percent
m	meter
m/s	meters per second
m^2/s^2	square meters per square second
mm	millimeter

CHAPTER 1 INTRODUCTION

Hydraulic structures can effectively break longitudinal habitat connectivity for aquatic organisms, either intentionally or inadvertently. Intentional barriers are typically put in place by managers to prevent invasive species introduction or hybridization (Holthe et al. 2005; Fausch et al. 2006). However, barriers are more frequently created simply because facilitating fish passage was not considered when the structure was designed and installed. Thus, anthropogenic obstructions have resulted in the fragmentation of waterways across the world (Williams et al. 2012). Longitudinal habitat connectivity is imperative for a successful life-cycle for migratory fish species (Schlosser and Angermeier 1995). Delays or terminations to upstream movement can negatively affect populations and disrupt ecosystem functions (Beechie et al. 2010).

Channel-spanning hydraulic structures continue to be emplaced in streams and rivers without being thoroughly evaluated for their effects on fish passage (Cada 1998; Noonan et al. 2012). However, as awareness of the issues associated with river fragmentation increases, a paradigm shift is occurring in the way fish passage concerns are addressed throughout the design process (Katopodis and Williams 2012). Upstream movement needs of potamodromous species are being considered with increasing importance (Santos et al. 2012; Silva et al 2012), although non-salmonid species are often neglected in favor of species with higher economic value (Katopodis 2005; Roscoe and Hinch 2010). Natural resource managers are frequently asked to comment on and permit proposed hydraulic structures (Kondratieff 2015) and, during this review process, engineers and scientists may be asked to provide model-based evidence of expected fish passage performance for their designs. While several methods of assessing and prioritizing existing hydraulic structures in regards to fish passage are currently available (Kemp et al. 2010),

an accurate and practicable tool is needed which can also assess the passage efficiency of proposed structures at this critical point prior to approval and installation.

Previous work focused on addressing this need has shown that 3D hydraulic modeling techniques can adequately resolve the complex hydrodynamics of channel-spanning structures for the purposes of assessing upstream fish movement (Stephens 2014). While these novel 3D analysis methods can be highly effective, with upwards of 80% overall prediction accuracy (Stephens 2014), developing a 3D computational fluid dynamics (CFD) model is time and resource intensive. The need for additional data collection, software licensing, modeling expertise, etc. can render 3D analysis impractical for many river management decisions. Practicing engineers and scientists are more likely to have the capacity for 2D hydraulic modeling for most hydraulic structure projects as various 2D model platforms have been used extensively for estimating flood discharges (Horritt and Bates 2002; Merwade et al. 2008) and evaluating in-stream fish habitat (Clark et al. 2008; Katopodis 2012). Although practical comparisons of 2D and 3D hydraulic models have been reported (Lane et al. 1999; Shen and Diplas 2008; Kolden 2013), studies which investigated the efficacy of 2D and 3D model-based assessments for fish passage were not found in the current literature.

1.1 Objectives

To make the highly effective 3D method of Stephens (2014) more accessible to natural resource managers and design engineers, this study investigates the feasibility of using a freely available, industry standard 2D CFD model, River2D (Steffler and Blackburn 2002), to evaluate the effects of a hydraulic structure on fish passage. Based on a similar approach, and using previous hydraulic and fish movement data sets (Fox 2013; Kolden 2013; Stephens 2014), this

study uses a 2D analysis method to assess a whitewater park (WWP) structure on the St. Vrain River at Lyons, CO. The specific objectives of this study are:

1. Develop a 2D CFD model that describes the complex hydraulic environment at the WWP structure.
2. Use the results of this 2D CFD model to create continuous, spatially explicit hydraulic descriptions along potential fish movement paths through the WWP structure.
3. Determine which hydraulic variables are most strongly associated with available fish movement data for rainbow trout (*Oncorhynchus mykiss*) and brown trout (*Salmo trutta*).
4. Compare the predictive assessment abilities, based on movement data from Passive Integrated Transponder (PIT)-tag studies, of the previously developed 3D approach (Stephens 2014) with the 2D approach of this study.
5. Provide recommendations to assist natural resource managers and designers with cost-effective assessments of hydraulic structures from the perspective of fish passage.

1.2 Background

A barrier to upstream fish movement can be created by a variety of physical conditions, including: flow depth, flow velocity, or a combination of flow velocity and distance (Coffman 2005; Cahoon et al. 2005). A depth barrier is typically created when the flow depth is too shallow to allow for passage attempts. Depth barriers can also exist when the drop height and/or plunge pool depth of a perched structure do not allow for passage due to leaping constraints. A velocity barrier is created when flow velocities exceed the swimming capabilities of fish trying to pass the structure, thus inhibiting upstream progress. An exhaustive barrier occurs at a structure when a combination of velocity and distance cause the fish to fatigue before successful

passage can be realized. The turbulence created by hydraulic structures can also play a role in fish passage. Depending on the conditions, turbulence can have both positive and negative effects on fish swimming (Liao 2007; Cotel and Webb 2012; Lacey et al. 2012).

Swimming performance metrics are often used to assess whether an existing hydraulic structure is acting as a barrier for fish passage. The most common of these metrics are burst swimming speeds, also known as sprinting speeds, and endurance curves (Castro-Santos et al. 2013). Fish exhibit three modes of swimming: sustained, prolonged, and burst (Peake et al. 1997). Sustained swimming can theoretically be maintained indefinitely, but prolonged and burst swimming speeds can only be maintained for limited amounts of time. Endurance curves are created by describing the inverse relationship between swimming velocity and fatigue time in a continuous manner over the three swimming modes (Videler and Wardle 1991). Burst swimming speeds are useful when identifying velocity barriers (Haro et al. 2004) and endurance curves help identify potential exhaustive barriers (Castro-Santos et al. 2013). At present, physical relationships between fish swimming performance and turbulence thresholds or distributions are not well understood (Liao 2007). However, some proxy variables such as total kinetic energy (TKE), total hydraulic strain, Reynolds shear stress, and vorticity have been shown to be useful when quantifying the effects of turbulence on fish (Nestler et al. 2008; Cotel and Webb 2012; Lacey et al. 2012; Silva et al. 2012).

Barriers can be complete, allowing no fish passage, or partial where selective passage success depends on physiological or hydraulic characteristics. For the purpose of this study, passage efficiency at the population level, based on the number of successful passes relative to the total number of attempts, will be used to quantify the extent of upstream movement suppression caused by the hydraulic structure (Haro et al. 2004). Various methods have been

developed to quantify how barriers are affecting fish passage (Kemp and O'Hanley 2010). One approach is to use statistical models, which allow for passage efficiency estimates to be represented on a continuous scale from 0 to 100 percent. In the past, rule-based or regression techniques have been used to assess culverts (Coffman 2005; Burford et al. 2009), road crossings (Warren and Pardew 1998), or flume experiment setups (Haro et al. 2004) with varying success. The statistical methods are able to combine information for hydraulic variables at varying scales to identify variables that strongly influence passage (Kemp and O'Hanley 2010). These models can also be validated using field based fish movement observations (Coffman 2005; Burford 2009). In 2014, Stephens developed a novel statistical method that utilized 3D CFD model outputs (Kolden 2013) to create a continuous, spatially explicit analysis method for assessing fish passage at hydraulic structures. The method was validated with field-collected hydraulic measurements and PIT-tag passage observations (Fox 2013) from three wave-creating, manmade whitewater park (WWP) structures in Colorado. The statistical results indicated that the Stephens (2014) method could predict passage efficiency with upwards of 80% overall accuracy.

While Stephens used results from a 3D CFD model, other studies have focused on describing complex flow at a scale relevant to fish with 2D CFD models (Lane et al. 1999; Crowder and Diplas 2000; Shen and Diplas 2008). The main concern with 2D CFD modeling has been whether the complexity associated meso-scale features important to fish habitat and swimming performance can be captured (Crowder and Diplas 2000). Mixed results show that, depending on the nature of the reach being modeled for habitat evaluation, 2D CFD models may or may not provide an appropriate description of hydraulic conditions (Clark et al. 2008; Shen and Diplas 2008; Kozarek et al. 2010). With a habitat or geomorphology modeling focus, the use of 3D models has been preferred when directly compared with depth averaged 2D models (Lane

et al. 1999; Shen and Diplas 2008). However, very few if any studies have comparatively evaluated the performance of 2D and 3D models when applied to the assessment of upstream fish movement at a hydraulic structure.

The comparison of CFD models in this study focuses on the 2D software River2D and the 3D software FLOW-3D (Flow Science, 2009). A chief difference between 2D and 3D models is that 2D models depth-average the values of hydraulic variables at each computational node. This depth-averaging has the potential to exclude important flow features and boundary layer effects that may strongly influence the fish-friendliness of a structure. For instance, a depth-averaged velocity value may erroneously suggested that hydraulic conditions downstream of a WWP structure are similar to those in a natural pool within the same reach, when in reality the two flow fields have unique characteristics that may affect fish populations differently (Kolden 2013). River2D also assumes hydrostatic pressure and a constant horizontal velocity distribution while FLOW-3D can avoid these assumptions. The hydrostatic pressure assumption, required by most 2D CFD modeling programs (Toombes and Chanson 2011), limits the computational accuracy across steep slopes (>10%) and rapidly changing slopes (Steffler and Blackburn 2002). The assumption that velocity distributions are constant, implying that vertical velocity components are negligible, essentially removes the capability of analyzing secondary flows and strong circulations with 2D CFD models (Steffler and Blackburn 2002; Toombes and Chanson 2011). Given these assumptions and the simplified nature of a 2D physical representation, it is unclear whether a 2D CFD model can adequately resolve the complex hydrodynamics of a channel-spanning structure for the predictive assessment of fish passage.

CHAPTER 2 METHODS

2.1 Site Description

The WWP structure analyzed in this study was one of nine that were constructed in 2003 on the North Fork of the St. Vrain River at Lyons, CO. The North Fork of the St. Vrain flows east from the Rocky Mountains and can be considered a transition zone from step-pool to pool-riffle within the study reach. Natural channel substrate consists of cobbles and boulders with a 1% channel slope. A typical snowmelt regime results in peak flows occurring from late May to early June. United States Geological Survey (USGS) stream gages exist both downstream and upstream of the Lyons WWP. The downstream gage is below the confluence with the South Fork and the upstream gage is near the outlet of Button Rock Reservoir. Therefore, a local stage-discharge rating curve was developed to allow for more accurate flow estimates (Fox 2013).

The complete Lyons WWP spanned a 400-m reach that flowed through Meadow Park; however, the structures were washed out during a September 2013 flood event. The peak runnable flow of this WWP on the St. Vrain River was around 14 cms, making it relatively small when compared to other popular WWPs in Colorado such as those in Salida (Arkansas River), 40 cms; Glenwood Springs (Colorado River), 570 cms; or Buena Vista (Arkansas River), 70 cms (RipBoard 2015). Three of the Lyons WWP structures were examined in previous studies using field-collected hydraulic conditions and fish movement observations (Fox 2013; Kolden 2013; Stephens 2014). The most downstream of these three structures, noted as WWP1 in prior studies, is further examined here. This structure used large un-grouted boulders to create a short, steep drop into a downstream pool.

2.2 Species of Interest

Four species of fish were PIT-tagged and monitored for movement through the Lyons WWP over 14 months (Fox 2013): brown trout (*Salmo trutta*), rainbow trout (wild *Oncorhynchus mykiss* and hatchery *Hofer x Harrison* strain), longnose dace (*Rhinichthys cataractae*), and longnose sucker (*Catostomus catostomus*). Due to a statistically insignificant number of observations for the native longnose dace and longnose sucker, only rainbow trout and brown trout data are used in this analysis. A total of 204 fish movement observations, 54 successful passes and 150 unsuccessful attempts were used for analysis at this WWP structure. Of these observations, 80 were brown trout (mean TL $\pm$ standard deviation, 209 $\pm$ 50 mm) and 124 were rainbow trout (mean TL $\pm$ standard deviation, 164 $\pm$ 20 mm). The observation sub-set is based on event filtering performed by Stephens (2014) for four discrete time windows within the overall observation period.

2.3 Hydraulic Modeling

In order to comparatively assess the suppression of fish passage using a 2D approach as opposed to a 3D approach, this analysis was based on the same hydraulic field measurements and topographical survey data used in Stephens (2014). A multi-step process based on the methods of Stephens (2014) was developed to create a hydraulic model and access the necessary variable output values. First, topography information was reformatted to a useable dataset, a River2D model was then calibrated, streamlines were extracted from this model, and finally hydraulic variable values specific to each point along the streamlines were compiled. The following sections further describe these steps.

2.3.1 Topography

In preparation for developing the River2D model, topography files were created by altering the input files used by Kolden (2013) for a 3D CFD model. Four stereolithography (STL) files comprising a 50-m reach around the WWP structure of interest were manually edited to decrease point density. First, vertical walls, substructures, and overhangs were removed. Point density was then further decreased by treating the remaining vertices as a landscape and selecting points to retain based on what features might be considered important to collect while surveying with a total station or Global Position System (GPS) instrument (i.e. breaks in slope, tops and bottoms of prominent features, etc.). This method allowed for variable densities throughout the reach and simulated methods that would likely be used to collect topography information when assessing other hydraulic structures in the future. The topography files were then imported into ArcMap™ v. 10.2 where the vertices were converted to points (ESRI [Environmental Systems Resource Institute] 2014). Values for x-coordinate, y-coordinate, and elevation of the points in each of the four portions were merged into a single text file for the study reach.

2.3.2 Model Development

The public domain River2D program suite was used to create a depth-averaged finite element hydrodynamic model of the WWP structure at four discharges: 0.42, 0.85, 1.70, and 2.83 cms. These four discharges encompass the range of flows at which fish movements were observed. The River2D model was calibrated at 0.79 cms using four velocity point measurements and 16 depth measurements taken along the channel thalweg. Three iterations of changing mesh spacing and 33 iterations of changing bed roughness by region were used during the initial calibration process. These simulations were evaluated using mean absolute error (MAE) values for velocity magnitude and flow depth (Lacey and Millar 2004). The top three

performing simulations, based on minimum MAE for depth and velocity combined, were used in a second calibration stage. At this point, the second eddy viscosity term, ε_2, of the River2D flow options was altered iteratively from 0.2 to 1.0 (Lacey and Millar 2004; Kozarek et al 2010). This parameter is a bed shear term and has been shown to be somewhat sensitive in models with instream obstructions (Kozarek et al 2010). While the River2D model was sensitive to iterating values of ε_2, the default value of 0.50 minimized MAEs. The best performing simulation from this second phase of calibration was considered the final 0.79 cms model (hereafter referred to as 0.85 cms to remain consistent with labels used in 3D analyses [Kolden 2013; Stephens 2014]). Bed and mesh files from this model were used for solving the 0.42, 1.70, and 2.83 cms models. Specifics regarding the final model parameters are provided in Appendix A.

River2D calibration resulted in an MAE of 63% for depth (45 mm), and 38% for velocity magnitude (0.40 m/s) across the 3.35 m sub-reach. Combined, this yields an overall MAE of 50% for the final 0.85 cms model. These errors, primarily the depth MAE, are greater than those reported in the literature for other River2D models (Kozarek et al. 2010; Lacey and Millar 2004). While an increase in velocity error was expected when moving to a depth-averaged model, the River2D depth error is also slightly larger than that reported for the 3D model of this WWP (Kolden 2013). An investigation into the errors showed that a topographical discrepancy, likely attributed to smoothing and bias associated with decreasing the original point density, was detected for the crest of the structure's drop feature. Flow depths at the crest of this structure were also difficult to calibrate in the 3D CFD model (Kolden 2013). When this problematic location was not considered, the depth MAE decreased sharply to 12% (33 mm) over the 3.35-m sub-reach. When the entire 50-m modeled reach was considered without the immediate crest region, the depth MAE was 14% (52 mm). The 12% and 14% depth MAEs are within the range

reported in the literature for other River2D models (Kozarek et al. 2010; Lacey and Millar 2004). Based on this information, the depth and velocity magnitude MAEs of the final 0.85 cms model were considered acceptable.

2.3.3 Streamline Extraction

The solved River2D models were opened in River2D Morphology v. 7.81. This related program supports a larger variety of file types and was used to output results as scalar time-series (TS3) files. The TS3 files were used with Blue Kenue™ to extract streamlines in lieu of emitting particle traces (Stephens 2014). Blue Kenue™ is public domain software for post-processing hydraulic models (Canadian Hydraulics Centre of the National Research Council Canada 2011). The x-velocity (U) and y-velocity (V) scalar files were combined to create a UV velocity vector layer. The "live cursor" tool was then used to trace and save points along a streamline. Streamlines were collected across a 3.35-m reach surrounding the WWP structure. This sub-reach was chosen to match the flow field defined by Stephens (2014). The extraction process was repeated using a negative UV velocity vector layer to simulate downstream emitted particle traces and better describe eddy zones downstream of the WWP structure. The number of streamlines extracted for each flow rate ranged from 800 to 1,800; further details on streamline extraction are provided in Appendix A.

2.3.4 Hydraulic Variable Outputs

For each modeled discharge, River2D results for depth, velocity magnitude, *x* discharge intensity, and *y* discharge intensity were exported as a grid with 12.7 mm spacing. Discharge intensity, more commonly referred to as unit discharge, is the discharge per unit width as described by Equation 1 and Equation 2:

$$q_x = HU \quad \textbf{Equation 1}$$

$$q_y = HV \quad \textbf{Equation 2}$$

where q_x and q_y are x discharge intensity and y discharge intensity, respectively, H is flow depth, and U and V are the x- and y-velocity components, respectively (Steffler and Blackburn 2002). Each output variable was turned into a raster with a cell size of 12.7 mm using ArcMap™. The x and y discharge intensities were divided by the depth raster to isolate the x- and y-velocity components in rasters of their own. Values from the depth, velocity magnitude, x-velocity component, and y-velocity component rasters were extracted and added to the attribute tables for each remaining point.

2.4 Particle Trace Evaluation

A portion of the streamlines, or particle traces, extracted in Blue Kenue™ did not span the entire 3.35 m sub-reach due to recirculation or termination in near zero velocity regions. To resolve this issue, incomplete particle traces were connected to the nearest complete trace. Recirculating traces were split at the point where recirculation began and attached to complete traces moving in same direction (downstream or upstream). This method of developing complete particle traces throughout the entire flow field is further explained in Stephens (2014). Each of the final complete particle traces was considered a potential path for fish to traverse when attempting to pass the WWP structure. Although fish may choose a physical path which crosses multiple traces when attempting passage, the assumption of particle traces as potential movement paths allows for a probabilistic representation of passable conditions throughout the flow field. In order to describe the conditions a fish would encounter while swimming along these potential movement paths, hydraulic variables describing flow depth, velocity, turbulence, and combined depth and velocity effects were quantified at each point along the trace.

2.4.1 Depth

Based on Stephens (2014), a particle trace was originally considered passable if the minimum depth along the trace was greater than 0.18 m. The fraction of impassable traces was then calculated to quantify what portion of the flow field was unavailable for potential upstream movement based on the minimum depth criterion (MDC). Preliminary 2D analysis also suggested that an MDC of 0.11 m ($MDC_{0.11}$) be evaluated. The 3D study method was re-evaluated using MDC values of 0.12, 0.11, 0.09, and 0.08 m. These additional 3D calculations allowed for direct 2D comparison and further explored the effects of using an MDC value less than the 0.18 m reported in Stephens (2014). Based on results of this preliminary work, all further analysis was conducted using $MDC_{0.11}$ and $MDC_{0.18}$.

The MDC variable does not take into account fish body depth. Further investigation was required to determine whether a flow depth of 0.11 m was physically appropriate. Hotchkiss and Frei (2007) compiled flow depth requirements for fish passage from various states. Maine requires that water be at least 1.5 times as deep as the body depth. Alaska requires that flow depth be 2.5 times the height of caudal fin (Figure 1).

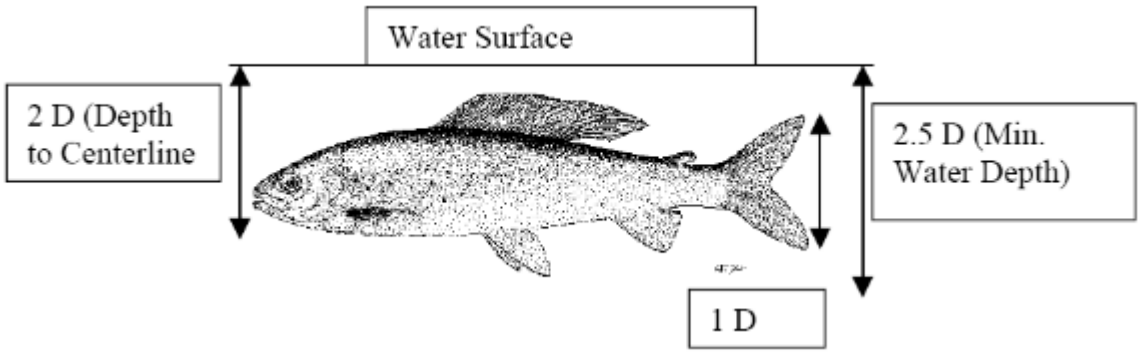

Figure 1. Alaska requires minimum water depth for fish passage to be 2.5 times the height of the caudal fin (D) (Hotchkiss and Frei 2007).

The fish movement observation data set used in this study only has a record of fish body length, as body depth and caudal fin height are not typical field measurements. Therefore, the following morphometric relationships (Equation 3 and Equation 4; Naeem 2002) were used to compare a flow depth of 0.11 m to the Alaska and Maine flow depth requirements:

$$TiW = 0.115 + 0.260TL \quad \textbf{Equation 3}$$

$$BD = -0.586 + 0.304TL \quad \textbf{Equation 4}$$

where TiW is the height of the caudal fin, BD is body depth, and TL is total length; all variables in centimeters. These relationships were developed by measuring 84 domestic rainbow trout.

Because a study reporting relationships between body length, body depth, and caudal fin height specifically for brown trout was not found in the literature, the mean body length of the entire study population (198 mm) was used to estimate a mean caudal fin height and mean body depth. This was considered an acceptable approach because intraspecific variation of rainbow trout physiology is likely just as large as the potential intraspecific variation between rainbow trout and brown trout (Myrick 2015). According to the morphometric calculations, the mean caudal fin height of the combined rainbow trout and brown trout observations at this WWP would be approximately 53 mm high. The mean body depth would be approximately 54 mm. Therefore, a minimum flow depth of 0.11 m would meet the Maine requirement of 1.5 times the body depth (0.08 m) but is slightly lower than the 2.5 times the caudal fin height required for fish passage by Alaska (0.13 m). Based on this information, it was determined that a flow depth of 0.11 m likely does cover the body and fins of the study population and thus allow for full swimming performance to be realized. Results using $MDC_{0.11}$ were considered physically practical and have been reported along with the $MDC_{0.18}$ results for both 2D and 3D analysis methods.

2.4.2 Velocity

The velocity magnitude output by River2D is the root-mean-square (rms) of the x- and y-velocity components. Because a magnitude value is always positive, it does not inherently incorporate direction. Therefore, a direction of flow (positive downstream) was assigned to the rms value based on the x-velocity component (Equation 5). In the case of strictly lateral flow, where the x-velocity component is absent, the rms value was kept positive.

$$v_{rms} = \sqrt{U^2 + V^2} \times \left(\frac{|U|}{U}\right) \quad \textbf{Equation 5}$$

Flow velocity was further described in a manner relative to fish swimming capabilities. A ratio of the water velocity and burst swimming velocity, v_{burst}, was computed (Equation 6):

$$\text{velocity ratio} = \frac{v_{rms}}{v_{burst}} \quad \textbf{Equation 6}$$

If the value of this ratio is ≥ 1, it suggests that fish cannot make upstream progress and a velocity barrier is present. The maximum value of this velocity ratio (MVR) along a trace was identified and if ≥ 1, the trace was considered impassable. The fraction of impassible traces was then calculated to quantify what portion of the flow field was unavailable for potential upstream movement based on MVR.

Swimming performance is directly related to fish body length (Bainbridge 1958; Videler and Wardle 1991; Ojanguren and Braña 2003). To capture this relationship, both the v_{rms} and v_{burst} values were converted from m/s to BL/s for each observed fish. Brown trout can reach sprinting speeds up to, and perhaps exceeding, 25 BL/s (Castro-Santos 2013). At present, swimming capability studies for rainbow trout report a maximum swimming speed of approximately 10 BL/s (Peake et al. 1997; Bainbridge 1960, sensu Castro-Santos 2013). However, studies indicate that burst swimming speeds are underestimated by respirometer

performance tests and rainbow trout can likely exceed 10 BL/s (Castro-Santos 2013; Tudorache et. al. 2010). Based on this information, MVR was computed using both 10 BL/s (MVR_{10}) and 25 BL/s (MVR_{25}) for size classes ranging from 100-400 mm with 25 mm increments. Including two v_{burst} estimates also helps capture some of the fitness and swimming performance variability of individuals within the study population (Williams et al. 2012).

2.4.3 Depth and Velocity Combination

Depth and velocity criteria were also combined into a single variable. A combined variable is better able to capture the variation in passage suppression associated with a depth and/or a velocity barrier being present at the WWP structure. The fraction of impassible traces was then calculated to quantify what portion of the flow field was unavailable for potential upstream movement based on both MDC and MVR. This computation was made for all four combinations of MDC (0.18 m or 0.11 m) and MVR (v_{burst} value of 25 BL/s or 10 BL/s).

2.4.4 Turbulence

In this 2D analysis, turbulence is quantified using a proxy variable to describe the fluctuations of velocity in space. This variable was modeled after the equation for turbulent kinetic energy (TKE), which is a measure of how kinetic energy changes as a result of velocity fluctuations and has been shown to be useful in predicting favorable hydraulic conditions for both rainbow trout and brown trout (Cotel and Webb 2012). The proxy 2D value describing spatial velocity fluctuations, v_{fluc}, was calculated as follows (Equation 7):

$$v_{fluc} = \frac{1}{2}(\sigma_u^2 + \sigma_v^2) \qquad \textbf{Equation 7}$$

where σ_u and σ_v are the standard deviations of the x- and y-velocity components, respectively, along the length of a potential movement path. The maximum value of v_{fluc} along a particle

trace was recorded as well as the sum of v_{fluc} for all points along a trace in an attempt to capture cumulative effects. In the 3D analysis, maximum TKE and the sum of TKE along a trace were used as proxy variables to describe the effects of turbulence on fish passage.

2.5 Statistical Analysis

A Boolean variable for successful/unsuccessful passage, body length, and the discharge conditions associated with successful passage attempts were taken from the fish movement observations and paired with the appropriate hydraulic conditions (Stephens 2014). A successful passage attempt was paired with the modeled discharge closest to the observed discharge. An unsuccessful passage attempt was paired with the modeled discharge closest to the discharge that most frequently occurred during the observation event period. The final assemblage of fish movement and hydraulic data was analyzed in the statistical program JMP® Pro 11 to identify which hydraulic variables were significant indicators of fish passage (SAS Institute Inc., 2013).

Standard regression diagnostics including a combination of forward and backward stepwise regression, with a stopping rule based on minimum Akaike Information Criterion (AIC), and a bivariate fit table were used to inform which variables should be included in the statistical analysis. The resulting manually chosen variables were fit to the fish movement observations using a logistic regression model. Several iterations of logistic regression models were analyzed to explore the strength of various hydraulic variables on their own in addition to multi-variable combinations. In this manner, the most parsimonious model could be identified. For comparative purposes, statistical models including the same hydraulic variables reported by Stephens (2014) were also analyzed. Model performance was measured using the resulting contingency tables to assess the overall passage prediction accuracy.

CHAPTER 3 RESULTS

3.1 Hydraulic Analysis

A comparison of 2D and 3D analysis methods at the downstream Lyons WWP structure identified nuances between the techniques over a range of discharges and fish size classes. The 2D results are based on River2D model outputs that provide spatially explicit values for flow depth and velocity while providing a means of visualizing potential passage routes via contour plots (Figure 2, 0.42 cms; , Figure 3 0.85 cms). The 3D results are based on those reported by Stephens (2014) and the additional 3D analysis performed during this study to investigate the effects of using $MDC_{0.11}$ as opposed to $MDC_{0.18}$.

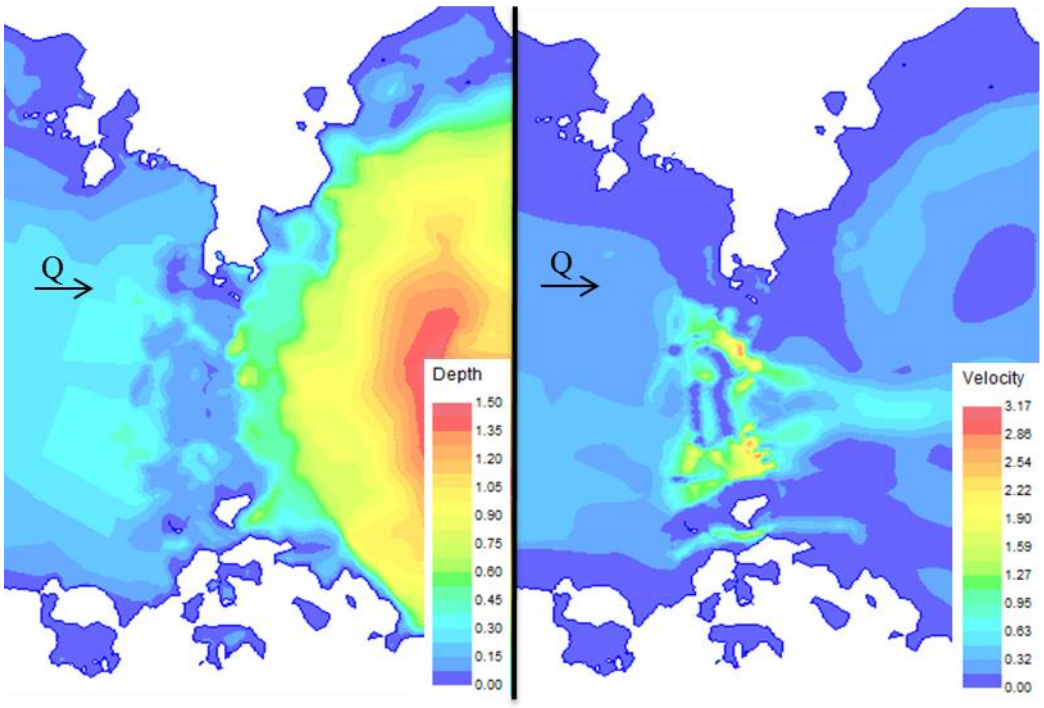

Figure 2. Depth (m) and velocity magnitude (m/s) River2D contours for 0.42 cms.

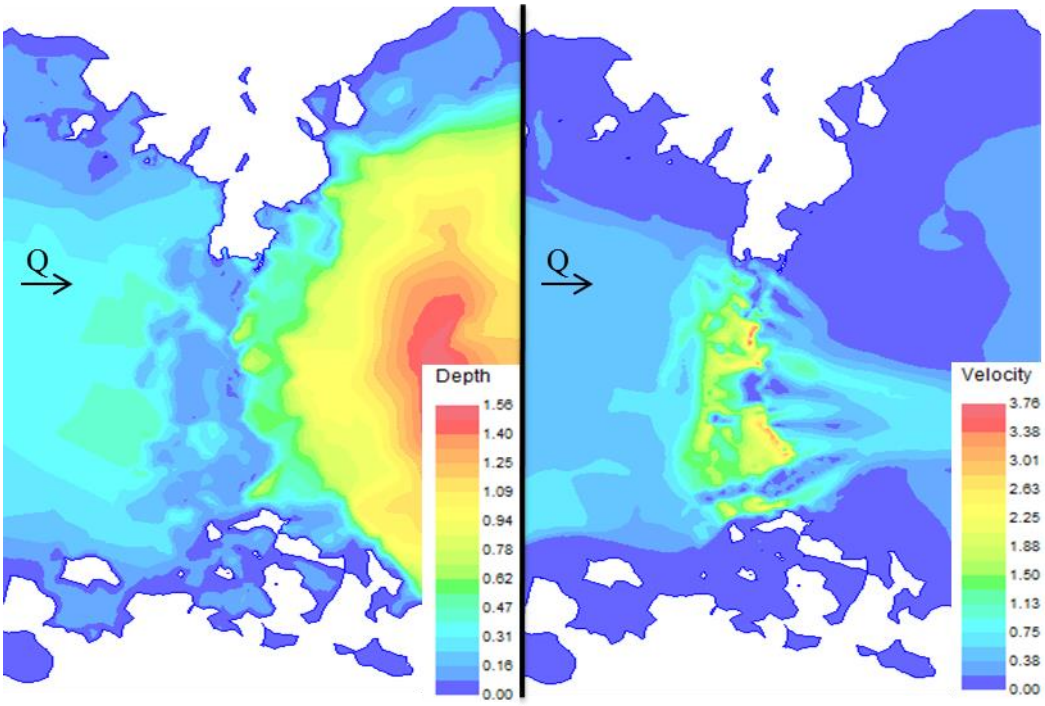

Figure 3. Depth (m) and velocity magnitude (m/s) River2D contours for 0.85 cms.

3.1.1 Depth

Using the 2D analysis method captures the general trend that as flow rate increases, the fraction of traces which do not provide adequate flow depth to support fish passage decreases (Figure 4). However, the 3D analysis method suggests that at a discharge of 1.70 cms a spike in inaccessible movement paths occurs at this structure. The 3D method also consistently suggests that more potential movement paths are available than the 2D results indicate. As expected, a larger MDC value yields fewer passable movement paths for both analysis methods.

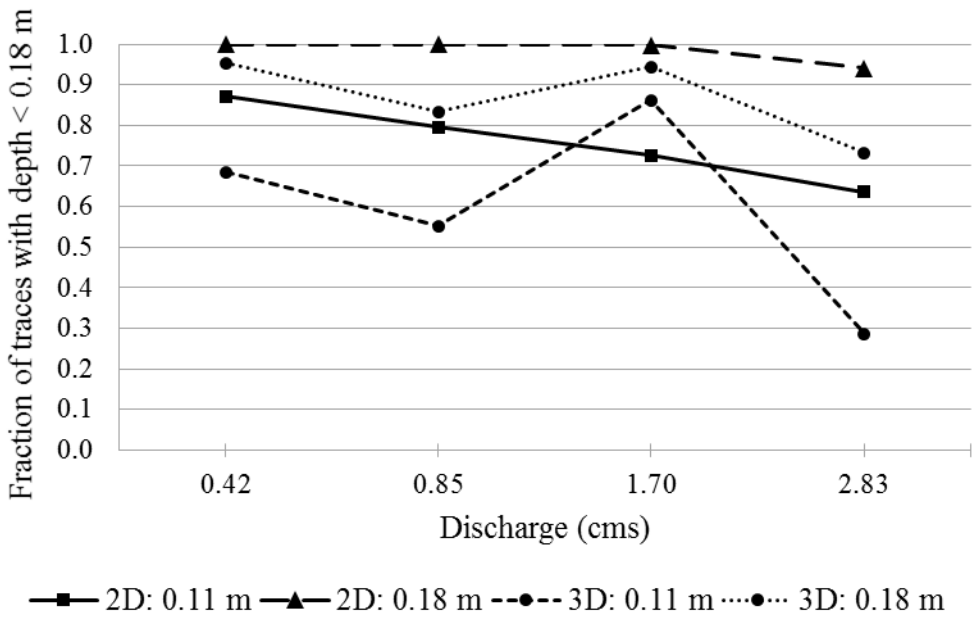

Figure 4. Fraction of potential movement paths that are impassable based on MDC values for both 3D and 2D analysis methods.

3.1.2 Velocity

The fraction of potential movement paths that are impassable due to the flow velocity being greater than a fish's burst swimming capability varies both with discharge, affecting the flow velocity, and fish body length, affecting swimming capability. For example, a 250-mm fish has a smaller portion of the flow field accessible for passage, based on MVR, at 2.83 cms than at 0.42 cms. However, a smaller 150-mm fish experiences the opposite effect and has more movement paths available at the higher discharge. These subtleties are quantified for both 2D and 3D analysis methods using MVR_{10} (Table 1) and MVR_{25} (Table 2). Differences in the fraction of flow field considered impassable between analysis methods are highlighted for both MVR values in Table 3.

Contrary to the MDC results, the 2D method consistently suggests that more movement paths are available than the 3D results indicate. With MVR_{10}, the 3D analysis suggests that no fish smaller than 200-mm can pass the structure at any discharge. The 2D analysis suggests that passage is possible to some extent for all size classes at all modeled discharges. With MVR_{25}, the 2D results show that the full flow field becomes accessible to the full range of size classes at the lowest discharge, while the 3D results suggest that the full flow field is more accessible to all fish at the highest modeled discharge. As expected, a smaller estimate of burst swimming speed yields fewer accessible movement paths for both analysis methods. When v_{burst} is 25 BL/s, the 2D and 3D results are identical for fish >250 mm, but the 2D results suggest more potential movement paths are available for smaller fish (Table 3). When v_{burst} is 10 BL/s, all size classes have more of the flow field available for passage in the 2D analysis; but this discrepancy in passable conditions between methods is again greater for the smaller bodied fish.

Table 1. Fraction of potential movement paths exceeding a burst swimming capability of 10 BL/s for each size class, discharge, and analysis method (black (1) = none available, white (0) = all available).

		Fish body length												
	Discharge (cms)	100 mm	125 mm	150 mm	175 mm	200 mm	225 mm	250 mm	275 mm	300 mm	325 mm	350 mm	375 mm	400 mm
2D	0.42	0.55	0.48	0.44	0.36	0.33	0.20	0.13	0.13	0.07	0.01	0	0	0
	0.85	0.67	0.65	0.53	0.42	0.37	0.27	0.21	0.15	0.08	0.03	0	0	0
	1.70	0.75	0.64	0.44	0.44	0.42	0.39	0.34	0.27	0.19	0.11	0.08	0.03	0
	2.83	0.56	0.54	0.36	0.31	0.30	0.28	0.27	0.25	0.23	0.19	0.15	0.10	0.05
3D	0.42	1	1	1	1	1	0.93	0.89	0.75	0.53	0.16	0.12	0.12	0.11
	0.85	1	1	1	1	1	1	1	0.75	0.58	0.39	0.20	0.12	0.09
	1.70	1	1	1	1	1	1	1	0.99	0.96	0.26	0.17	0.13	0.12
	2.83	1	1	1	1	1	1	1	1	0.96	0.93	0.62	0.21	0.12
	Ranges:	1		0.99 - 0.80		0.79 - 0.60		0.59 - 0.40		0.39 - 0.20		0.19 - 0.01		0

Table 2. Fraction of potential movement paths exceeding a burst swimming capability of 25 BL/s for each size class, discharge, and analysis method (black (1) = none available, white (0) = all available).

		Fish body length												
	Discharge (cms)	100 mm	125 mm	150 mm	175 mm	200 mm	225 mm	250 mm	275 mm	300 mm	325 mm	350 mm	375 mm	400 mm
2D	0.42	0.13	0	0	0	0	0	0	0	0	0	0	0	0
	0.85	0.21	0.05	0	0	0	0	0	0	0	0	0	0	0
	1.70	0.34	0.15	0.03	0	0	0	0	0	0	0	0	0	0
	2.83	0.27	0.21	0.10	0.01	0	0	0	0	0	0	0	0	0
3D	0.42	0.89	0.20	0.12	0.07	0.02	0.02	0	0	0	0	0	0	0
	0.85	1	0.44	0.12	0.08	0.01	0	0	0	0	0	0	0	0
	1.70	1	0.25	0.13	0.06	0.05	0	0	0	0	0	0	0	0
	2.83	1	0.95	0.21	0.07	0	0	0	0	0	0	0	0	0
	Ranges:	1		0.99 - 0.80		0.79 - 0.60		0.59 - 0.40		0.39 - 0.20		0.19 - 0.01		0

Table 3. Difference in fraction of impassable potential movement paths based on MVR between 2D and 3D analysis methods. Negative values (italicized) indicate that more paths are considered available by the 2D analysis method and vice versa.

		Fish body length												
	Discharge (cms)	100 mm	125 mm	150 mm	175 mm	200 mm	225 mm	250 mm	275 mm	300 mm	325 mm	350 mm	375 mm	400 mm
MVR_{10}	0.42	*-0.45*	*-0.52*	*-0.56*	*-0.64*	*-0.67*	*-0.73*	*-0.76*	*-0.62*	*-0.46*	*-0.15*	*-0.12*	*-0.12*	*-0.11*
	0.85	*-0.33*	*-0.35*	*-0.47*	*-0.58*	*-0.63*	*-0.73*	*-0.79*	*-0.60*	*-0.50*	*-0.36*	*-0.20*	*-0.12*	*-0.09*
	1.70	*-0.25*	*-0.36*	*-0.56*	*-0.56*	*-0.58*	*-0.61*	*-0.66*	*-0.72*	*-0.77*	*-0.15*	*-0.09*	*-0.10*	*-0.12*
	2.83	*-0.44*	*-0.46*	*-0.64*	*-0.69*	*-0.70*	*-0.72*	*-0.73*	*-0.75*	*-0.73*	*-0.74*	*-0.47*	*-0.11*	*-0.07*
MVR_{25}	0.42	*-0.76*	*-0.20*	*-0.12*	*-0.07*	*-0.02*	*-0.02*	0	0	0	0	0	0	0
	0.85	*-0.79*	*-0.39*	*-0.12*	*-0.08*	*-0.01*	0	0	0	0	0	0	0	0
	1.70	*-0.66*	*-0.10*	*-0.10*	*-0.06*	*-0.05*	0	0	0	0	0	0	0	0
	2.83	*-0.73*	*-0.74*	*-0.11*	*-0.06*	0	0	0	0	0	0	0	0	0
	Ranges:	1		0.99 - 0.80		0.79 - 0.60		0.59 - 0.40		0.39 - 0.20		0.19 - 0.01		0

3.1.3 Depth and Velocity Combination

The fraction of potential movement paths that are impassable due to a combination of depth and velocity criteria is also dependent on both discharge and fish body length. These subtleties are quantified in Tables 4 through 7 for four combinations of MDC (0.11 m and 0.18

m) and MVR (using 10 BL/s and 25 BL/s). Differences in the fraction of flow field considered impassable between 2D and 3D analysis method are highlighted for each variable combination in Table 8. As expected, increasing the burst swimming speed estimate increases the portion of the flow field considered available for successful passage. Similarly, decreasing the MDC value decreases the amount of potential movement paths that are impassable. Unlike when depth and velocity are analyzed separately, there is not a consistent relationship between the 2D and 3D analysis methods for the combined depth and velocity variables. In general, the 2D analysis method suggests more movement paths are available with MVR_{10} than the 3D method indicates for fish less than 300 mm in length, especially with $MDC_{0.11}$, and vice versa for size classes larger than 300 mm (Table 8). With MVR_{25}, the 3D analysis method generally suggests that more movement paths are available for all size classes compared to the 2D method (a key exception being the 1.70 cms results). However, results for all four combined variables are relatively quite similar between the 2D and 3D analysis methods, with a mean of 0.06 for the difference in fraction of flow field considered impassable.

With $MDC_{0.11}$ and MVR_{10}, almost no movement paths are available to fish smaller than 300 mm, especially when utilizing the 3D analysis method (Table 4). In general, the passable portion of flow field increases with discharge for the 2D analysis. More of the flow field becomes passable when the MVR is changed to reflect a burst swimming speed of 25 BL/s (Table 5). This combination, still using an $MDC_{0.11}$, generally yields a positive relationship between discharge and the amount of available movement paths. Again, a key exception is the spike in unavailable movement paths at 1.70 cms in the 3D analysis method.

Table 4. Fraction of potential movement paths with a minimum depth less than 0.11 m and/or exceeding a burst swimming capability of 10 BL/s for each size class, discharge, and analysis method (black (1) = none available, white (0) = all available).

		Fish body length												
	Discharge	100	125	150	175	200	225	250	275	300	325	350	375	400
	(cms)	mm	mm	mm	mm	mm	mm	mm	mm	mm	mm	mm	mm	mm
2D	0.42	0.97	0.97	0.97	0.97	0.97	0.96	0.95	0.94	0.88	0.87	0.87	0.87	0.87
	0.85	0.95	0.95	0.95	0.95	0.94	0.90	0.88	0.86	0.83	0.81	0.80	0.80	0.80
	1.70	0.94	0.94	0.94	0.94	0.94	0.94	0.92	0.89	0.84	0.80	0.78	0.74	0.73
	2.83	0.86	0.86	0.86	0.86	0.85	0.85	0.85	0.84	0.83	0.80	0.76	0.73	0.68
3D	0.42	1	1	1	1	1	0.98	0.98	0.98	0.95	0.82	0.69	0.68	0.68
	0.85	1	1	1	1	1	1	1	0.98	0.94	0.79	0.65	0.62	0.61
	1.70	1	1	1	1	1	1	1	1	0.98	0.96	0.89	0.88	0.87
	2.83	1	1	1	1	1	1	1	1	0.97	0.94	0.75	0.45	0.37
	Ranges:	1		0.99 - 0.80		0.79 - 0.60		0.59 - 0.40		0.39 - 0.20		0.19 - 0.01		0

Table 5. Fraction of potential movement paths with a minimum depth less than 0.11 m and/or exceeding a burst swimming capability of 25 BL/s for each size class, discharge, and analysis method (black (1) = none available, white (0) = all available).

		Fish body length												
	Discharge	100	125	150	175	200	225	250	275	300	325	350	375	400
	(cms)	mm	mm	mm	mm	mm	mm	mm	mm	mm	mm	mm	mm	mm
2D	0.42	0.95	0.87	0.87	0.87	0.87	0.87	0.87	0.87	0.87	0.87	0.87	0.87	0.87
	0.85	0.88	0.83	0.80	0.80	0.80	0.80	0.80	0.80	0.80	0.80	0.80	0.80	0.80
	1.70	0.92	0.82	0.75	0.73	0.73	0.73	0.73	0.73	0.73	0.73	0.73	0.73	0.73
	2.83	0.85	0.82	0.73	0.64	0.64	0.64	0.64	0.64	0.64	0.64	0.64	0.64	0.64
3D	0.42	0.98	0.72	0.68	0.68	0.68	0.68	0.68	0.68	0.68	0.68	0.68	0.68	0.68
	0.85	1	0.83	0.62	0.60	0.56	0.55	0.55	0.55	0.55	0.55	0.55	0.55	0.55
	1.70	1	0.98	0.88	0.87	0.86	0.86	0.86	0.86	0.86	0.86	0.86	0.86	0.86
	2.83	1	0.96	0.45	0.34	0.29	0.29	0.29	0.29	0.29	0.29	0.29	0.29	0.29
	Ranges:	1		0.99 - 0.80		0.79 - 0.60		0.59 - 0.40		0.39 - 0.20		0.19 - 0.01		0

Increasing the minimum depth to $MDC_{0.18}$ decreases the number of available movement paths for both MVR_{10} and MVR_{25} across all discharges and both analysis methods. Using the 2D method, $MDC_{0.18}$ combined with MVR_{10} (Table 6) eliminates potential passage across discharges of 0.42, 0.85, and 1.70 cms and less than six percent of the flow field is available at 2.83 cms.

Using the 3D analysis method, movement paths become available across all discharges for size classes greater than 300 mm. When $MDC_{0.18}$ is combined with MVR_{25} (Table 7), the 2D results remain the same as when combined with MVR_{10}. However, with the 3D analysis method, fish greater than 125 mm TL see an increase in passable movement paths across all discharges.

Table 6. Fraction of potential movement paths with a minimum depth less than 0.18 m and/or exceeding a burst swimming capability of 10 BL/s for each size class, discharge, and analysis method (black (1) = none available, white (0) = all available).

		Fish body length												
	Discharge (cms)	100 mm	125 mm	150 mm	175 mm	200 mm	225 mm	250 mm	275 mm	300 mm	325 mm	350 mm	375 mm	400 mm
2D	0.42	1	1	1	1	1	1	1	1	1	1	1	1	1
	0.85	1	1	1	1	1	1	1	1	1	1	1	1	1
	1.70	1	1	1	1	1	1	1	1	1	1	1	1	1
	2.83	0.98	0.98	0.98	0.98	0.98	0.98	0.98	0.98	0.98	0.96	0.95	0.94	0.94
3D	0.42	1	1	1	1	1	1	1	1	0.96	0.95	0.95	0.95	0.95
	0.85	1	1	1	1	1	1	1	1	1	0.97	0.88	0.88	0.87
	1.70	1	1	1	1	1	1	1	1	1	0.99	0.95	0.95	0.95
	2.83	1	1	1	1	1	1	1	0.99	0.99	0.96	0.67	0.39	0.37
	Ranges:	1		0.99 - 0.80		0.79 - 0.60		0.59 - 0.40		0.39 - 0.20		0.19 - 0.01		0

Table 7. Fraction of potential movement paths with a minimum depth less than 0.18 m and/or exceeding a burst swimming capability of 25 BL/s for each size class, discharge, and analysis method (black (1) = none available, white (0) = all available).

		Fish body length												
	Discharge (cms)	100 mm	125 mm	150 mm	175 mm	200 mm	225 mm	250 mm	275 mm	300 mm	325 mm	350 mm	375 mm	400 mm
2D	0.42	1	1	1	1	1	1	1	1	1	1	1	1	1
	0.85	1	1	1	1	1	1	1	1	1	1	1	1	1
	1.70	1	1	1	1	1	1	1	1	1	1	1	1	1
	2.83	0.98	0.97	0.94	0.94	0.94	0.94	0.94	0.94	0.94	0.94	0.94	0.94	0.94
3D	0.42	1	0.95	0.95	0.95	0.95	0.95	0.95	0.95	0.95	0.95	0.95	0.95	0.95
	0.85	1	0.98	0.88	0.87	0.83	0.83	0.83	0.83	0.83	0.83	0.83	0.83	0.83
	1.70	1	1	0.95	0.95	0.95	0.95	0.95	0.95	0.94	0.94	0.94	0.94	0.94
	2.83	1	0.99	0.78	0.73	0.73	0.73	0.73	0.73	0.73	0.73	0.73	0.73	0.73
	Ranges:	1		0.99 - 0.80		0.79 - 0.60		0.59 - 0.40		0.39 - 0.20		0.19 - 0.01		0

Table 8. Difference in fraction of impassable potential movement paths based on combined MDC & MVR between 2D and 3D analysis methods. Negative values (italicized) indicate that more paths are considered available by the 2D analysis method and vice versa.

		Fish body length												
	Discharge (cms)	100 mm	125 mm	150 mm	175 mm	200 mm	225 mm	250 mm	275 mm	300 mm	325 mm	350 mm	375 mm	400 mm
$MDC_{0.11}$ & MVR_{10}	0.42	***-0.03***	***-0.03***	***-0.03***	***-0.03***	***-0.03***	***-0.02***	***-0.03***	***-0.04***	***-0.07***	0.05	0.18	0.19	0.19
	0.85	***-0.05***	***-0.05***	***-0.05***	***-0.05***	***-0.06***	***-0.10***	***-0.12***	***-0.12***	***-0.11***	0.02	0.15	0.18	0.19
	1.70	***-0.06***	***-0.06***	***-0.06***	***-0.06***	***-0.06***	***-0.06***	***-0.08***	***-0.11***	***-0.14***	***-0.16***	***-0.11***	***-0.14***	***-0.14***
	2.83	***-0.14***	***-0.14***	***-0.14***	***-0.14***	***-0.15***	***-0.15***	***-0.15***	***-0.16***	***-0.14***	***-0.14***	0.01	0.28	0.31
$MDC_{0.11}$ & MVR_{25}	0.42	***-0.03***	0.15	0.19	0.19	0.19	0.19	0.19	0.19	0.19	0.19	0.19	0.19	0.19
	0.85	***-0.12***	0.0	0.18	0.20	0.24	0.25	0.25	0.25	0.25	0.25	0.25	0.25	0.25
	1.70	***-0.08***	***-0.16***	***-0.13***	***-0.14***	***-0.13***	***-0.13***	***-0.13***	***-0.13***	***-0.13***	***-0.13***	***-0.13***	***-0.13***	***-0.13***
	2.83	***-0.15***	***-0.14***	0.28	0.30	0.35	0.35	0.35	0.35	0.35	0.35	0.35	0.35	0.35
$MDC_{0.18}$ & MVR_{10}	0.42	0	0	0	0	0	0	0	0	0.04	0.05	0.05	0.05	0.05
	0.85	0	0	0	0	0	0	0	0	0	0.03	0.12	0.12	0.13
	1.70	0	0	0	0	0	0	0	0	0	0.01	0.05	0.05	0.05
	2.83	***-0.02***	***-0.02***	***-0.02***	***-0.02***	***-0.02***	***-0.02***	***-0.02***	***-0.01***	***-0.01***	0	0.28	0.55	0.57
$MDC_{0.18}$ & MVR_{25}	0.42	***-0.03***	0.15	0.19	0.19	0.19	0.19	0.19	0.19	0.19	0.19	0.19	0.19	0.19
	0.85	***-0.12***	0	0.18	0.20	0.24	0.25	0.25	0.25	0.25	0.25	0.25	0.25	0.25
	1.70	***-0.08***	***-0.16***	***-0.13***	***-0.14***	***-0.13***	***-0.13***	***-0.13***	***-0.13***	***-0.13***	***-0.13***	***-0.13***	***-0.13***	***-0.13***
	2.83	***-0.15***	***-0.14***	0.28	0.30	0.35	0.35	0.35	0.35	0.35	0.35	0.35	0.35	0.35
	Ranges:	1		0.99 - 0.80		0.79 - 0.60		0.59 - 0.40		0.39 - 0.20		0.19 - 0.01		0

3.1.4 Turbulence

In the 2D analysis, the largest values of v_{fluc}, both at an individual point and summed along the trace, occurred at the lowest modeled discharge. In general, the water appears to have become somewhat less turbulent as the flow rate increased (Figure 5). However, a majority of the flow field experiences similar v_{fluc} values across all discharges. The 2D maximum v_{fluc} results were similar to the maximum TKE values from the 3D analysis; however, the sums of TKE values were one to two orders of magnitude larger than the summed v_{fluc} values used to describe cumulative turbulence effects in the 2D analysis (Stephens 2014).

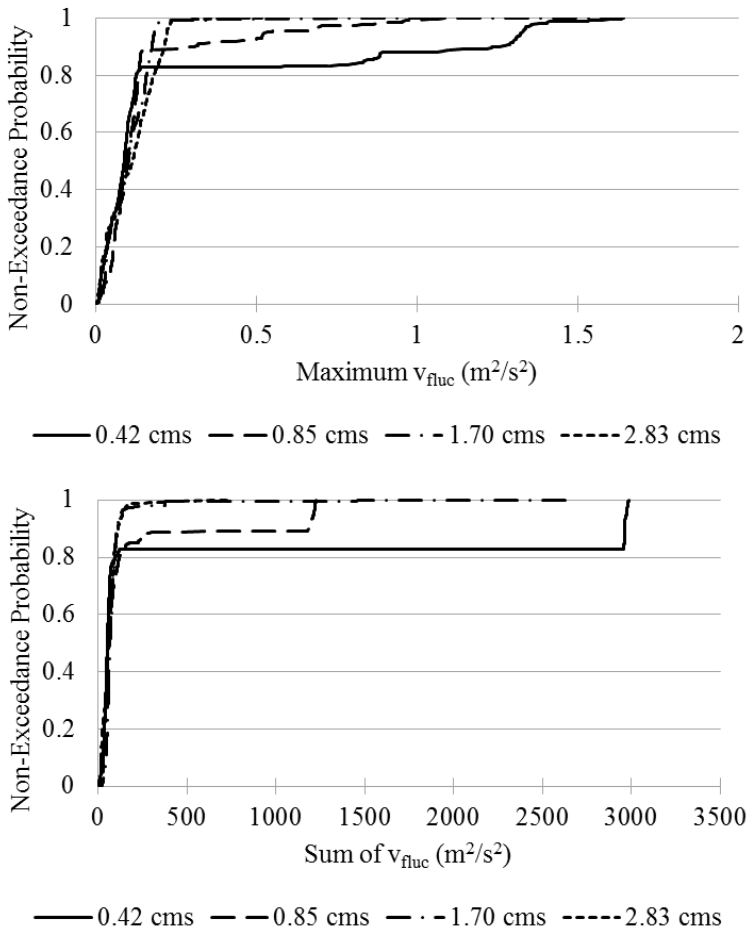

Figure 5. Non-exceedance probabilities for the maximum v_{fluc} and sum of v_{fluc} along particle traces for each discharge as modeled in River2D.

3.2 Statistical Analysis

The MDC and MVR variables were consistently identified as the strongest predictors of fish passage. In the 3D analysis (Stephens 2014), $MDC_{0.11}$ (Table 9) predicted observations with the same accuracy as $MDC_{0.18}$ (Table 10). Additional 3D analysis showed that a model with an MDC of 0.12 m performed the same (91.2% accuracy) as $MDC_{0.18}$ and $MDC_{0.11}$. However, once the MDC was lowered to 0.09 m and 0.08 m, prediction accuracy dropped sharply. In the 2D

analysis, $MDC_{0.11}$ (Table 9) accurately predicted 92.2% of fish movement observations while $MDC_{0.18}$ (Table 10) yielded 75.5% prediction accuracy.

Logistic regression was also performed for the combined MDC and MVR variables. In both analyses, MVR_{25} predicted the successful movement attempts better than MVR_{10}. A slight decrease in the prediction of unsuccessful movements occurred with MVR_{25} in the 3D analysis, but overall prediction was about 15% more accurate than MVR_{10} (Tables 9 and 10). There was a similar difference in the overall predictive strength of the MVR_{10} and MVR_{25} combined variables with the 2D analysis.

Table 9. Observed and predicted frequencies of successful passage attempts using $MDC_{0.11}$, the combined $MDC_{0.11}$ & MVR_{10}, and the combined $MDC_{0.11}$ and MVR_{25} for both 2D and 3D analysis methods.

2D Analysis						3D Analysis					
			Predicted						Predicted		
		Observed	Pass	No Pass	% Correct			Observed	Pass	No Pass	% Correct
$MDC_{0.11}$		Pass	46	8	85.2%	$MDC_{0.11}$		Pass	44	10	81.5%
		No Pass	8	142	94.7%			No Pass	8	142	94.7%
		Overall % Correct			92.2%			Overall % Correct			91.2%
$MDC_{0.11}$	& MVR_{10}	Pass	4	50	7.4%	$MDC_{0.11}$	& MVR_{10}	Pass	0	54	0.0%
		No Pass	8	142	94.7%			No Pass	0	150	100.0%
		Overall % Correct			71.6%			Overall % Correct			73.5%
$MDC_{0.11}$	& MVR_{25}	Pass	45	9	83.3%	$MDC_{0.11}$	& MVR_{25}	Pass	40	14	74.1%
		No Pass	8	142	94.7%			No Pass	8	142	94.7%
		Overall % Correct			91.7%			Overall % Correct			89.2%

Table 10. Observed and predicted frequencies of successful passage attempts using $MDC_{0.18}$, the combined $MDC_{0.18}$ & MVR_{10}, and the combined $MDC_{0.18}$ and MVR_{25} for both 2D and 3D analysis methods.

2D Analysis					3D Analysis				
		Predicted					Predicted		
	Observed	Pass	No Pass	% Correct		Observed	Pass	No Pass	% Correct
$MDC_{0.18}$	Pass	4	50	7.4%	$MDC_{0.18}$	Pass	44	10	81.5%
	No Pass	0	150	100.0%		No Pass	8	142	94.7%
	Overall % Correct			75.5%		Overall % Correct			91.2%
$MDC_{0.18}$ & MVR_{10}	Pass	2	52	3.7%	$MDC_{0.18}$ & MVR_{10}	Pass	0	54	0.0%
	No Pass	0	150	100.0%		No Pass	0	150	100.0%
	Overall % Correct			74.5%		Overall % Correct			73.5%
$MDC_{0.18}$ & MVR_{25}	Pass	4	50	7.4%	$MDC_{0.18}$ & MVR_{25}	Pass	43	11	79.6%
	No Pass	0	150	100.0%		No Pass	8	142	94.7%
	Overall % Correct			75.5%		Overall % Correct			90.7%

Decreasing the minimum flow depth to 0.11 m did not significantly affect the 3D analysis prediction results, but did greatly increase the 2D prediction accuracies for both the independent MDC and the combined MDC & MVR models. Based on these results, $MDC_{0.11}$ was considered to be a stronger assessment variable than the deeper $MDC_{0.18}$ used by Stephens (2014). Table 11 provides a more in-depth examination of the following statistical models: $MDC_{0.11}$, $MDC_{0.11}$ & MVR_{10}, $MDC_{0.11}$ & MVR_{25}.

Table 11. Logistic regression analysis summary for $MDC_{0.11}$, the combined $MDC_{0.11}$ & MVR_{10}, and the combined $MDC_{0.11}$ & MVR_{25} for both 2D and 3D analysis methods.

	Predicted logit of (passage success) =	Likelihood ratio test (p -value)	Goodness-of-fit test (p -value)	Parameter Estimate (p -value)	Odds ratio (e^{β})		Observations accurately predicted (overall %)
2D Analysis	(-48.57) + 58.99*$MDC_{0.11}$	< 0.0001	< 0.0001	< 0.0001	$MDC_{0.11}$	4.17E+25	92.2
	(-29.61) + 32.11*$MDC_{0.11}$&MVR_{10}	< 0.0001	< 0.0001	< 0.0001	$MDC_{0.11}$ & MVR_{10}	8.78E+13	71.6
	(-48.57) + 58.97*$MDC_{0.11}$&MVR_{25}	< 0.0001	0.899	< 0.0001	$MDC_{0.11}$ & MVR_{25}	4.07E+25	91.7
3D Analysis	16.61 + (-27.75)*$MDC_{0.11}$	< 0.0001	< 0.0001	< 0.0001	$MDC_{0.11}$	8.91E-13	91.2
	(-4.33) + 3.34*$MDC_{0.11}$&MVR_{10}	0.3483	0.0828	0.3982	$MDC_{0.11}$ & MVR_{10}	28.35003	73.5
	20.92 + (-33.22)*$MDC_{0.11}$&MVR_{25}	< 0.0001	< 0.0001	< 0.0001	$MDC_{0.11}$ & MVR_{25}	3.73E-15	89.2

In the 3D analysis, both the $MDC_{0.11}$ and the combined $MDC_{0.11}$ & MVR_{25} models have goodness-of-fit test results that suggest the model could be improved by including additional variables ($p < 0.05$). However, for each of these models the likelihood ratio test results show that the current variables are predicting fish passage with significant accuracy ($p < 0.05$). The $MDC_{0.11}$ & MVR_{10} model does not perform well as indicated by both the likelihood ratio test *(p* > 0.05) and parameter estimate *p*-value ($p > 0.05$), but the goodness-of-fit test suggests that adding more variables would not improve that performance ($p > 0.05$). In the 2D analysis, all of the final models are predicting fish passage with high accuracy ($p < 0.05$), but the goodness-of-fit test results suggest that additional variables could further improve the performance of the $MDC_{0.11}$ and $MDC_{0.11}$ & MVR_{10} models. Both analysis methods suggest MDC is more influential than MVR, when these variables are considered alone, on fish passage success (unit

odds ratio = 4.17×10^{25}, 2D; 8.91×10^{-13}, 3D). However, the 3D analysis suggests a negative relationship while the 2D analysis suggests a positive relationship, as indicated by the sign of the exponent. From the final selection of models, the 2D depth-only model, $MDC_{0.11}$, performs best with an overall prediction accuracy of 92.2%. This model performs slightly (~1%) better than the best model reported in Stephens (2014), also the depth-only model, for this particular structure. The improvement is due to a slightly higher accuracy in predicting the successful passage attempts with the 2D analysis method.

CHAPTER 4 DISCUSSION

4.1 Comparison of the 2D and 3D Analysis Methods

The overall accuracy of predicting fish movement observations (Table 11) was comparable between the 2D and 3D analysis methods when $MDC_{0.11}$ was used in place of the original $MDC_{0.18}$ as recommended by Stephens (2014). Both analyses suggest that the Lyons WWP structure is acting as a partial barrier to fish passage and strongly suppressing upstream movement. Differences between the methods did emerge when breaking down the fraction of available movement paths by discharge and fish size class. In general, with the combined depth and velocity variables, the 2D method suggests that more passable movement paths are available for smaller fish (< 300 mm) than the 3D method, and vice versa for larger fish (Table 8). The combined depth and velocity models from the 2D method, with $MDC_{0.11}$, predict the amount of successful passage attempts more accurately than the 3D method (Table 9). As the majority of those successful passage observations were smaller fish, the slightly increased prediction accuracy of the 2D models is likely attributed to the 2D method suggesting that more of the flow field is available for the passage of smaller fish. Still, results for all four combined variables are relatively quite similar between the 2D and 3D analysis methods, with a mean of 0.06 for the difference in fraction of flow field considered impassable.

These subtle discrepancies between analysis methods are most likely attributed to the depth-averaged nature of the 2D analysis. When considering depth, the 3D method accounts for multiple potential movement paths throughout the water column, capturing the idea that more of the flow area is accessible per unit width in deeper areas. The 2D method counts one potential movement path per unit width, regardless of flow depth relative to the MDC. When considering

velocity, if the depth-averaged velocity is passable, the 2D method considers the one potential movement path per unit width passable. The 3D method can capture regions where, for example, the average velocity may be passable but a significant portion of the water column consists of a high velocity jet that creates impassable hydraulic conditions. However, a precursory analysis that simply depth-averaged the 3D analysis results showed little to no change in prediction accuracy of most models. These preliminary results suggest that the difference in absolute number of traces between the 2D analysis method (10^3) and the 3D analysis method (10^4), primarily due to the increased number of particle traces in the vertical direction with the 3D method, is not strongly influencing overall prediction at the Lyons WWP structure. This conclusion, albeit structure-specific, is also supported by the minor differences in prediction accuracy between the 2D and 3D analysis methods.

There are scenarios that may lie outside the range of physical conditions in which the 2D analysis method can provide realistic approximations of the fraction of flow field with impassable hydraulic conditions. Relatively small, but important regions of passable conditions, such as those produced by boundary layer effects, may be washed out when hydraulic variables are depth-averaged. For example, available passage routes along the bed or along structure edges may not be resolved through deep waters where a majority of the water column has velocities that exceed the burst swimming capabilities of fish. Conversely, very shallow depths with a strong submerged jet may average the region of impassable conditions out and erroneously suggest that a structure is fish-friendly when it is actually a barrier. Structures that pose a stronger potential for being depth barriers are expected to have a wider range for feasible 2D assessment. This is because the depth-averaging of the 2D analysis method primarily affects estimates of the impassable fraction of a flow field based on MVR, not MDC. When considering

whether a 2D analysis method is reasonable for a particular hydraulic structure, care should be taken to regard the regions where movement may be physically inhibited with most importance, i.e. the chute of a WWP and not the downstream pool where fish are merely approaching the structure prior to actively attempting passage. Physical conditions which violate key assumptions in 2D CFD modeling, such as steep slopes (>10%) or large radii of curvature (Steffler and Blackburn 2002; Toombes and Chanson 2011), should be assessed using a 3D analysis method.

4.2 Key Hydraulic Variables for Predicting Fish Passage

Logistic regression analysis consistently identified flow depth and velocity as the key predictors of fish passage at the WWP structure (Table 11). It is important to note that the velocity is not strictly the flow velocity, but the ratio of flow velocity to burst swimming speed in terms of fish body length, computed over several size classes. Additionally, the actual values going into the logistic regression models are not the raw flow depth or velocity ratios. The statistical analysis uses the fraction of potential movement paths, which were identified by extracting streamlines and considering each of those flow paths a potential route for fish attempting to pass the structure, that do not meet the MDC or MVR criteria.

At this particular structure, the MDC variable performed slightly better on its own (~1%) than when combined with the MVR variable. However, a combination of MDC and MVR is recommended for the assessment of hydraulic structures beyond this Lyons WWP structure. The physical nature of the downstream Lyons WWP, a short and steep chute that drops into a plunge pool, suggests that there is inherently more potential for a depth barrier to be created than a velocity barrier. The combined MDC and MVR variable only resulted in a minor loss of prediction accuracy at this depth-dominant structure. The comparable results suggest that a

combined depth and velocity variable can accurately capture both depth and velocity barriers and is thus a stronger indicator of fish passage suppression over a range of structure types.

Inclusion of the MVR variable highlights that estimates of the burst swimming capabilities, or sprinting speeds, for species of interest influence the model's performance. Care should be taken to use accurate v_{burst} estimates, and separate MVR values are recommended for species with significantly different swimming capabilities within the same study population. Turbulence, as described by the variable v_{fluc}, did not appear to significantly influence fish passage at this structure. While turbulent waters are likely affecting fish passage in some manner (Enders et al. 2005; Liao 2007), the chosen 2D proxy variable did not capture these effects.

4.3 Capturing Complex Flow with a 2D CFD Model

When including the immediate region surrounding the crest of the WWP structure, the final River2D calibration had relatively large depth and velocity magnitude MAEs. Nonetheless, each modeled discharge produces parameter estimates that are accurately predicting fish passage ($p < 0.05$) (Table 11). A topography discrepancy about the height of the chute crest appears to be contributing to the increased depth and velocity magnitude errors. If topography information had been collected with the specific intention of using it in a River2D model, calibration errors would likely decrease in magnitude.

Further support that a 2D CFD model may sufficiently capture complex flow nature for means of fish passage assessment comes from a visual inspection of the River2D outputs. At this particular structure, the boulders used to create the chute and drop were left un-grouted. Doing so created interstitial spaces that may be serving as flow refuges or alternate passage routes for smaller bodied fish (Stephens 2014). Approximately 60% of fish with TL < 200 mm successfully

passed, while only around 35% of larger fish were successful. The flows paths through these interstitial spaces appear to be at least partially resolved by the River2D model. Small, but generally continuous pockets of greater depth and lower velocity magnitude are visible in the contour displays (Figure 2, 0.42 cms; Figure 3, 0.85 cms) around the chute and drop region.

The interstitial flow path resolution and parameter estimate *p*-values indicate that the River2D model is sufficiently describing the complex flow at a hydraulic structure. However, a 2D CFD model assumes an essentially constant velocity distribution throughout the water column (Steffler and Blackburn 2002). This could potentially pose a problem when attempting to identify physical processes that are inhibiting upstream fish movement. Kolden (2013) provides an example of this weakness at a WWP structure located just upstream of the structure used in this 2D analysis. The upstream structure creates a submerged jet that reverses the natural flow conditions; velocities are now highest near the bed and slowest near the surface. However, when depth-averaged, the velocity magnitude erroneously suggests that flow conditions at the structure match those in a natural control reach. Fish species that are accustomed to taking advantage of lower velocity zones near the bed, and thus seek refuge or attempt passage near the bed, may experience a greater degree of suppression due to the atypical conditions surrounding a hydraulic structure (Kolden 2013). Fish populations that navigate turbulent waters in their natural environment, such as those in step-pool systems that exhibit naturally occurring hydraulic jumps, submerged jet flow, and recirculation (Thompson et al. 1998), may be better accustomed to the flow conditions produced by a hydraulic structure. Because 2D analysis methods are more likely to correctly identify physical processes that are limiting successful passage if the vertical velocity distribution is of less importance (Toombes and Chanson 2011), the likelihood that fish

attempting to pass the structure have experience swimming through a range of turbulent flows is an important consideration when interpreting results based on a 2D CFD model.

4.4 Recommendations for Fish Passage Assessment

The novel 3D hydraulic analysis method developed by Stephens (2014) provides an effective approach to evaluate the effects a hydraulic structure has on fish passage. The 2D analysis method developed in this study also offers a powerful technique for describing the hydraulic conditions at a structure and assessing the potential suppression of upstream fish movement. However, the 2D analysis employs a CFD modeling package, River2D, that has become an industry standard and is often favored by practitioners in North America (Bledsoe 2015). Both of the hydraulic modeling components of the 2D analysis method, River2D and Blue Kenue™, are public domain resources. The predilection to use River2D and the open source nature of the CFD software programs suggests that the 2D method may be more cost effective to implement (i.e. less demanding in data collection, software licensing, additional modeling expertise, etc.) and thus more readily accepted in practice.

The results of this study suggest that the 2D analysis method can be used to assess the effectiveness of similar hydraulic structures at both providing fish passage and serving as an intentional barrier. When selecting a final model to use where preserving longitudinal habitat connectivity is of importance, focus should be placed on the accuracy of the "no pass" prediction. These results will more conservatively assess the fish passage potential of the structure by emphasizing fish that were suppressed. In selecting a final model to use in designing protections against two populations mixing (i.e. protecting an upstream native population from the introduction of a downstream invasive species), focus should be placed on the accuracy of

the “pass” prediction. These results will more conservatively assess the effectiveness of a barrier by emphasizing the potential for fish to successfully pass upstream.

Fish are known to take advantage of lower velocity zones at the boundary layers of flow features (Fausch 1993; Williams et al. 2012). Interstitial spaces, like those left between boulders at the downstream Lyons WWP structure, can facilitate passage for smaller bodied fish which would likely not have been able to pass through the main velocity jet (Stephens 2014). Native, non-salmonid fish populations, which are often difficult to include in statistical analysis due to low observation numbers (Kondratieff 2015), could also be benefiting from interstitial spaces. These spaces may serve as alternate passage routes with lower flow velocities for some fish, or as refuge areas where energy can be restored before attempting the next leg of passage. Therefore, interstitial spaces are recommended for the design of channel spanning hydraulic structures. The size of these spaces should be large enough for the expected body sizes, considering both width and depth, of fishes that need to pass the structure. Flows paths through interstitial spaces and/or along a structure’s margins need to provide continuous corridors of passable conditions.

Based on the results of this study, a minimum flow depth of 0.11 m is recommend for passing adult trout. In the case of larger bodied fishes, different species, or different life-stages than the current study population, an alternate minimum depth may be required (Cahoon et al. 2007). Keeping the various species and life-stages of interest in mind, care should be taken that velocities (for at least a portion of the channel) do not exceed reasonable estimates of burst swimming speeds for the fishes with the lowest swimming capabilities. When passing adult trout, this study recommends using a burst swimming estimate of 25 BL/s. The expected body length of fish that need to pass a structure should be considered, and passable conditions

provided for a range of size classes. The development of a 2D CFD model, if 3D modeling resources are not feasible, and utilization of the analysis method presented in study (or that of Stephens (2014) if undertaking a 3D analysis), is recommended to assess whether a structure design will provide adequate fish passage prior to installation. Conducting this spatially explicit hydraulic analysis will allow for design alternatives to be ranked by fish passage performance and help identify any necessary design alterations.

4.5 Future Directions

As indicated by the goodness-of-fit test results (Table 11), additional variables could improve the overall model performance of this analysis ($p < 0.05$). The current assessment method does not appear to describe turbulence in a manner meaningful for fish. Perhaps using different proxy variables that better describe turbulence intensity, periodicity, orientation, and scale (IPOS) of vortices as relevant to fish would improve model performance (Lacey et al. 2012). However, even with a change in how turbulence is quantified, a 2D CFD model may not sufficiently represent the turbulent conditions. Hydraulic structures that produce considerable turbulence may be better assessed using a 3D CFD model. Adding behavioral variables to include an agent-based perspective (Haefner and Bowen 2002; Nestler et al. 2005; Goodwin et al. 2006), such as the strain-velocity-pressure hypotheses developed by Goodwin (2004) could also improve the assessment performance and better inform the design of future hydraulic structures. Even if behavior variables that reflect path choices are not included, the full extent of potential movement paths may be better described using a tree network to encompass all possible upstream steps from each position in the flow field. Finally, the model could be made more explicit by incorporating MDC and MVR variables relevant to each species of interest and computing species-specific passage rates rather than using aggregated information.

Future work regarding the assessment of hydraulic structures for fish passage extends beyond adding complexity to further improve the already effective 2D or 3D analysis methods. The 2D analysis was only performed on a single hydraulic structure. The 3D analysis was performed on three types of structures at a single WWP. More studies involving a larger variety of hydraulic structure types, larger/smaller scale rivers, different hydraulic regimes, and a wider range of fish species would greatly increase the strength of inferences made using both the 2D and 3D analysis methods. These studies should approach data collection with the intent of using it specifically in a 2D or 3D model-based assessment to allow for the maximum utilization of each method. Future studies would also help address remaining questions about the transferability of MDC and MVR results from this study to other structures. Additional field observations that provide more specific information on the lateral and vertical position of the paths fish are favoring while attempting passage would also be beneficial. The more spatially explicit observations, which could be made using above/below water video recording, would help inform behavioral rules and potentially identify the most pragmatic zones for increased hydraulic resolution (Nestler et al. 2008). From a physiological perspective, swimming performance metrics still need to be determined for many fish species, especially non-salmonids (Katopodis 2005; Furniss et al. 2006; Castro-Santos 2009).

CHAPTER 5 CONCLUSIONS

This study investigated the feasibility of using public domain 2D CFD modeling programs, which are commonly used in industry, to describe the complex flow at a hydraulic structure for purposes of assessing fish passage. River2D model results were used to compare a 2D continuous, spatially explicit hydraulic analysis method for predicting fish passage with a similar 3D method (Stephens 2014). Performance was measured using prediction accuracy based on field observations of brown trout and rainbow trout movement through a WWP structure in Lyons, CO. Results suggest that 2D CFD modeling can sufficiently resolve potential swimming paths through the structure. Logistic regression indicated that flow depth and velocity are strong predictors of how this hydraulic structure influences fish passage. Using a combined depth and velocity variable, the 2D analysis method accurately predicted 92% of fish movement observations at the Lyons WWP structure. The same combined variable had 90% accuracy with the 3D analysis method. The performance difference is due to slightly higher accuracy in predicting successful attempts with the 2D method. However, goodness-of-fit tests suggest that other physical processes, such as turbulence, and behavior choices are also contributing to the passage suppression at this structure. Further research is needed to allow for the inclusion of behavioral variables and provide accurate estimates of burst swimming capabilities for more fish species, especially non-salmonids. Additional studies utilizing the 2D and 3D analysis methods evaluated here will help address questions concerning the transferability of results to a variety of hydraulic structure types on waterways of varying scale. Nonetheless, this study supports the findings of Stephens (2014) that depth and velocity are key physical indicators of upstream movement suppression and offers a cost-effective assessment method for determining how a similar proposed hydraulic structure might affect fish passage prior to approval and installation.

CHAPTER 6 REFERENCES

Bainbridge, R. 1958. The speed of swimming of fish as related to size and to the frequency and amplitude of the tail beat. *J. Exp. Biol.* 35(1):109-33.

Bainbridge, R., 1960. Speed and stamina in three fish. *J. Exp. Biol.* 37(1):129-153.

Beechie, T. J., D. A. Sear, J. D. Olden, G. R. Pess, J. M. Buffington, H. Moir, P. Roni, and H. M. H. Pollock, 2010. Process-based principles for restoring river ecosystems. *BioScience* 60(3):209-222.

Bledsoe, B., 2015. Personal Communication, Colorado State University, Department of Civil and Environmental Engineering.

Burford, D. D., T. E. McMahon, J. E. Cahoon, and M. Blank, 2009. Assessment of Trout Passage through Culverts in a Large Montana Drainage during Summer Low Flow. *North American Journal of Fisheries Management* 29(3):739-52. DOI: 10.1577/M07-175.1.

Cada, G. F., 1998. Fish passage mitigation at hydroelectric power projects in the United States. In: *Fish Migration and Fish Bypasses*, Jungwirth, M., S. Schmutz, and S. Weiss (Editors). Fishing News Books, Oxford, pp. 208-219.

Cahoon, J. E., T. McMahon, O. Stein, D. Burford, and M. Blank, 2005. Fish passage at road crossings in a Montana watershed. Report No. FHWA/MT-05-002/8160, The State of Montana Department of Transportation, Helena, MT, 39 pp.

Cahoon, J. E., T. McMahon, A. Sokz, M. Blank, and O. Stein, 2007. Fish passage in Montana culverts: Phase II – Passage goals. Report No. FHWA/MT-07-010/8181, The State of Montana Department of Transportation, Helena, MT, 64 pp.

Canadian Hydraulics Centre of the National Research Centre, 2015. Blue Kenue Reference Manual, Ottawa, Ontario, Canada.

Castro-Santos, T., A. Cotel, and P. Webb, 2009. Fishway evaluations for better bioengineering: an integrative approach. In: *Challenges for Diadromous Fishes in a Dynamic Global Environment*, A. Haro et al. (Editors). Conference Proceedings, pp. 557-575.

Castro-Santos, T., F. J. Sanz-Ronda, and J. Ruiz-Legazpi, 2013. Breaking the speed limit – comparative sprinting performance of brook trout (*Salvelinus fontinalis*) and brown trout (*Salmo trutta*). *Can. J. Fish. Aquat. Sci.* 70(2):280-293. DOI: 10.1139/cjfas-2012-0186.

Clark, J. S., D. M. Rizzo, M. C. Watzin, and W. C. Hession, 2008. Spatial distribution and geomorphic condition of fish habitat in streams: An analysis using hydraulic modeling and geostatistics. *River. Res. Applic.* 24(7):885-889.

Coffman, J. S., 2005. Evaluation of a Predictive Model for Upstream Fish Passage through Culverts. Masters Thesis, James Madison University, Harrisonburg, VA.

Cotel, A. J. and P. W. Webb, 2012. The Challenge of Understanding and Quantifying Fish Responses to Turbulence-dominated Physical Environments. In: *Natural Locomotion in Fluids and on Surfaces*, S. Childress et al. (Editors). Springer Science+Business Media, New York, pp. 15-33.

Crowder, D. W. and P. Diplas, 2000. Using two-dimensional hydrodynamic models at scales of ecological importance. *Journal of Hydrology* 230(3-4):172-191.

Enders, E. C., D. Boisclair, and A. G. Roy, 2005. A model of total swimming costs in turbulent flow for juvenile Atlantic salmon (*Salmo salar*). *Can. J. Fish. Aquat. Sci.* 62(5):1079-1089.

ESRI (Environmental Systems Resource Institute), 2014. ArcMap™ 10.2. ESRI, Redlands, California.

Fausch, K. D., 1993. Experimental analysis of microhabitat selection by juvenile steelhead (*Oncorhynchus mykiss*) and coco salmon (*O. kisutch*) in a British Columbia stream. *Can. J. Fish. Aquat. Sci.* 50(6):1198-1207.

Fausch, K. D., B. E. Rieman, M. K. Young, and J. B. Dunham, 2006. Strategies for conserving native salmonid populations at risk from nonnative fish invasions: tradeoffs in using barriers to upstream movement. Gen. Tech. Rep. RMRS-GTR-174. U. S. Department of Agriculture, Forest Service, Rocky Mountain Research Station, Fort Collins, CO, 44 pp.

Flow Science, 2009. FLOW-3D User Manual: v9.4, Flow Science, Inc.

Fox, B., 2013. Eco-Hydraulic Evaluation of Whitewater Parks as Fish Passage Barriers. Masters Thesis, Colorado State University, Department of Civil and Environmental Engineering, Fort Collins, CO.

Furniss M., M. Love, S. Firor, K. Moynan, A. Llanos, J. Guntle, and R. Gubernick, 2006. FishXing Version 3.0, United States Forest Service, Corvallis, OR.

Goodwin, R. A., 2004. Hydrodynamics and Juvenile Salmon Movement Behavior at Lower Granite Dam: Decoding the Relationship using 3-D Space-Time (CEL Agent IMB) Simulation. Doctoral Dissertation, Cornell University, Ithaca, NY.

Goodwin, R. A., J. M. Nestler, J. J. Anderson, L. J. Weber, and D. P. Loucks, 2006. Forecasting 3-D fish movement behavior using a Eulerian-Lagrangian-agent method (ELAM). *Ecological Modelling* 192(1-2):197-223.

Haefner, J. W. and M. D. Bowen, 2002. Physical-based model of fish movement in fish extraction facilities. *Ecological Modelling* 152(2):227-245.

Haro, A., T. Castro-Santos, J. Noreika, and M. Odeh, 2004. Swimming performance of upstream migrant fishes in open-channel flow: a new approach to predicting passage through velocity barriers. *Can. J. Fish. Aquat. Sci.* 61(9):1591-1601.

Holthe, E., E. Lund, B. Finstad, E. B. Thorstad, and R. S. McKinley, 2005. A fish selective obstacle to prevent dispersion of an unwanted fish species, based on leaping capabilities. *Fisheries Management and Ecology* 12(2):143-147.

Horritt, M. S. and P. D. Bates, 2002. Evaluation of 1D and 2D numerical models for predicting river flood inundation. *Journal of Hydrology* 268(1-4):87-99.

Hotchkiss, R. H. and C. M. Frei, 2007. Design for Fish Passage at Roadway-stream Crossings: Synthesis Report. Publication No. FHWA-HIF-07-033, U. S. Department of Transportation, Federal Highway Administration, McLean, VA, June 280 pp.

Katopodis, C., 2005. Developing a toolkit for fish passage, ecological flow management, and fish habitat works. *Journal of Hydraulic Research* 43(5):451-467.

Katopodis, C., 2012. Ecohydraulic approaches in aquatic ecosystems: Integration of ecological and hydraulic aspects of fish habitat connectivity and suitability. Editorial, *Ecological Engineering* 48:1-7.

Katopodis, C. and J. G. Williams, 2012. The development of fish passage research in a historical context. *Ecological Engineering* 48:8-18.

Kemp, P. S. and J. R. O'Hanley, 2010. Procedures for evaluating and prioritising the removal of fish passage barriers: a synthesis. *Fisheries Management and Ecology* 17(4):297-322.

Kolden, E., 2013. Modeling in a Three-dimensional World: Whitewater Park Hydraulics and Their Impact on Aquatic Habitat in Colorado. Masters Thesis, Colorado State University, Department of Civil and Environmental Engineering, Fort Collins, CO.

Kondratieff, M., 2015. Personal Communication, Colorado Parks and Wildlife.

Kozarek, J. L., W. C. Hession, C. A. Dolloff, and P. Diplas, 2010. Hydraulic Complexity Metrics for Evaluating In-Stream Brook Trout Habitat. *J. Hydraul. Eng*. 136(12):1067-1076.

Lacey, R. W. J. and R. G. Millar, 2004. Reach Scale Hydraulic Assessment of Instream Salmonid Habitat Restoration. *Journal of the American Water Resources Association (JAWRA)* 40(6):1631-1644.

Lacey, R. W. J., V. S. Neary, J. C. Liao, E. C. Enders, and H. M. Tritico, 2012. The IPOS Framework: Linking Fish Swimming Performance in Altered Flows From Laboratory Experiments to Rivers. *River Res. Applic.* 28(4):429-443.

Lane, S. N., K. F. Bradbrook, K. S. Richards, P. A. Biron, and A. G. Roy, 1999. The application of computational fluid dynamics to natural river channels: three-dimensional versus two-dimensional approaches. *Geomorphology* 29(1-2):1-20.

Liao, J. C., 2007. A review of fish swimming mechanics and behaviour in altered flows. Philosophical Transactions of the Royal Society B: Biological Sciences 362(1487):1973-1993.

Merwade, V., A. Cook, and J. Coonrod, 2008. GIS techniques for creating river terrain models for hydrodynamic modeling and flood inundation mapping. *Environmental Modelling & Software* 23(10-11):1300-1311.

Myrick, C., 2015. Personal Communication, Colorado State University, Department of Fish, Wildlife, and Conservation Biology.

Naeem, M., 2002. Body composition, elemental concentration, and morphometrics of Rainbow trout (*Oncorhynchus mykiss*) and Big-head carp (*Aristichthys nobilis*) in Pakistan. Doctoral Thesis. Bahauddin Zakariya University, Institute of Pure and Applied Biology, Multan, Pakistan.

Nestler, J. M., R. A. Goodwin, and D. P. Loucks, 2005. Coupling of Engineering and Biological Models for Ecosystem Analysis. *J. Water Resour. Plann. Manage.* 131(2):101-109.

Nestler, J. M., R. A. Goodwin, D. L. Smith, J. J. Anderson, and S. Li, 2008. Optimum Fish Passage and Guidance Designs are Based in the Hydrogeomorphology of Natural Rivers. *River. Res. Applic.* 24(2):148-168.

Noonan, M. J., J. W. A. Grant, and C. D. Jackson, 2012. A quantitative assessment of fish passage efficiency. *Fish and Fisheries* 13:150-464.

Ojanguren, A. F. and F. Braña, 2003. Effects of size and morphology on swimming performance in juvenile brown trout (*Salmo trutta* L.). *Ecology of Freshwater Fish* 12(4):241-246.

Peake, S., R. S. McKinley, and D. A. Scruton, 1997. Swimming performance of various freshwater Newfoundland salmonids relative to habitat selection and fishway design. *J. Fish Biol.* 51(4):710-723.

RipBoard (2015). Whitewater parks and kayak play parks: great riverboarding near urban communities. RipBoard Inc., Denver, CO; available: www.ripboard.com/community/whitewaterpark.shtml.

Roscoe, D. W. and S. G. Hinch, 2010. Effectiveness monitoring of fish passage facilities: historical trends, geographic patterns and future directions. *Fish and Fisheries* 11:12-33.

SAS Institute Inc., 2013. Using JMP® 11. SAS Institute Inc., Cary, NC.

Santos, J. M., A. Silva, C. Katopodis, P. Pinheiro, A. Pinheiro, J. Bochechas, and M. T. Ferreira, 2012. Ecohydraulics of pool-type fishways: Getting past the barriers. *Ecological Engineering* 48:38-50.

Schlosser, I. J. and P. L. Angermeier, 1995. Spatial variation in demographic processes of lotic fishes: conceptual models, empirical evidence, and implications for conservations. *American Fisheries Society Symposium* 17:392-401.

Silva, A. T., C. Katopodis, J. M. Santos, M. T. Ferreira, and A. N. Pinheiro, 2012. Cyprinid swimming behavior in response to turbulent flow. *Ecological Engineering* 44:314-328.

Shen, Y. and P. Diplas, 2008. Application of two- and three-dimensional computational fluid dynamics models to complex ecological stream flows. *Journal of Hydrology* 348(1-2):195-214.

Steffler, P. and J. Blackburn, 2002. River2D Two-Dimensional Depth Averaged Model of River Hydrodynamics and Fish Habitat: Introduction to Depth Averaged Modeling and User's Manual, University of Alberta, Edmonton, Alberta, Canada.

Stephens, T., 2014. Effects of Whitewater Parks on Fish Passage: A Spatially Explicit Hydraulic Analysis. Masters Thesis. Colorado State University, Department of Civil and Environmental Engineering, Fort Collins, CO.

Thompson, D. M., J. M. Nelson, and E. E. Wohl, 1998. Interactions between pool geometry and hydraulics. *Water Resour. Res.* 34(12):3673-3681.

Toombes, L. and H. Chanson, 2011. Numerical Limitations of Hydraulic Models. The 34th International Association for Hydraulic Research World Congress, Brisbane, Australia, pp. 2322-2329.

Tudorache, C., P. Viaenen, R. Blust, and G. DeBoeck, 2007. Longer flumes increase critical swimming speeds by increasing burst and glide swimming duration in carp (*Cyprinus carpio,* L.). *J. Fish Biol.* 71(6):1630-1638.

Warren Jr., M. L. and M. G. Pardew, 1998. Road Crossings as Barriers to Small-Stream Fish Movement. *Transactions of the American Fisheries Society* 127(4):637-644.

Williams, J. G., G. Armstrong, C Katopodis, M. Larinier, and F. Travade, 2012. Thinking like a fish: A key ingredient for development of effective fish passage facilities at river obstructions. *River Res. Applic.* 28(4):407-417.

Videler, J. J. and C. S. Wardle, 1991. Fish swimming stride by stride: speed limits and endurance. *Rev. Fish Biol. Fish.* 1(1):23-40.

APPENDIX A HYDRAULIC ANALYSIS DETAILS

A.1 River 2D Model Development

A text file containing the topography information and an initial roughness height estimate, k_s, for each point was imported into R2D_bed v. 1.24. The resulting bed file was used in R2D_mesh v. 2.02 to create a triangular computational mesh with a total of 46,187 nodes. The mesh and bed files were then used in River2D v. 0.95a to solve for a steady-state solution. Inflow discharge was used as an upstream boundary and water surface elevation as a downstream boundary. River2D allows for solver and flow options to be adjusted from default values. In this study, the built-in Generalized Minimal Residual (GMRES) method iterative solver was used with an analytical Jacobian matrix (Steffler and Blackburn 2002). The following flow options were changed from default values to assist with solving at low flow depths: minimum depth for groundwater flow, 0.10; groundwater transmissivity, 0.01 (Steffler and Blackburn 2002; Kozarek et al 2010). After calibration was completed, the final bed file used the following regional values for roughness height, k_s: 0.001 upstream of the WWP structure, 15.5 just at the crest of the structure to capture the abrupt depth change, 0.0005 in the downstream pool, and all other areas kept at the initial estimate of 0.75. Final mesh spacing was a 0.50 uniform fill with a 0.10 region fill through the chute of the structure.

A.2 Streamline Extraction

When extracting streamlines in Blue Kenue™, the temporal scale of the live cursor varied between 0.005 and 1.5 seconds and the number of points collected along a streamline within this time frame varied between 800 and 2,500 as needed for adequate resolution. The

number of streamlines extracted, using both downstream and upstream techniques, are provided in Table 12.

Table 12. Number of streamlines extracted for each discharge.

Streamline Type	Discharge (cms)			
	0.42	0.85	1.70	2.83
Upstream	848	556	1127	863
Downstream	305	323	438	888
Total	1153	879	1565	1751

A.3 Particle Trace Evaluation

Hydraulic variable values were extracted from the River2D outputs and combined with the streamline point x- and y-coordinates in ArcMap™. The "Extract Multi Values to Point" tool was utilized, but required all streamline points falling within the bounds of the hydraulic variable rasters associated with the 3.35 m sub-reach. To accommodate this, an integer version of the depth raster was converted to a polygon to serve as a boundary for streamline points. Text files containing the streamline points were imported into ArcMap™ and clipped remove any points outside of the River2D output raster extents. Once extracting the values to the streamline points, the amended attribute tables were exported from ArcMap™ as text files to be used for further evaluation.

LIST OF ABBREVIATIONS

2D	two-dimensional
3D	three-dimensional
AIC	Akaike Information Criterion
CO	Colorado
CFD	computational fluid dynamics
CPW	Colorado Parks and Wildlife
GMRES	Generalized Minimal Residual
GPS	Global Positioning System
IPOS	intensity, periodicity, orientation, scale
MAE	mean absolute error
MDC	minimum depth criterion
$MDC_{0.11}$	minimum depth criterion of 0.11 m
$MDC_{0.18}$	minimum depth criterion of 0.18 m
MVR	maximum velocity ratio
MVR_{10}	maximum velocity ratio with v_{burst} estimate of 10 BL/s
MVR_{25}	maximum velocity ratio with v_{burst} estimate of 25 BL/s
PIT	passive integrated transponder
TKE	turbulent kinetic energy

TL	total length
™	trademark
TS3	time-series file type
USGS	United States Geological Survey
WWP	whitewater park